

Dual Energy CT: Demystified

Introduction to Dual Energy CT

Xinhui Duan, PhD, DABR

April, 2020
AAPM Spring Meeting



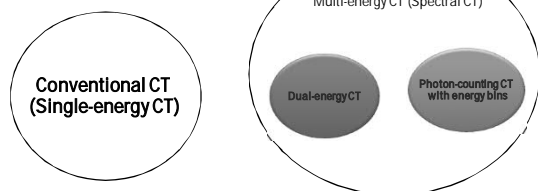
Learning Objective

- Understand the basic physics of dual-energy CT imaging.
- Learn about commercial dual-energy CT scanners and their pros and cons.
- Learn about common dual-energy CT clinical applications.

4/4/2020



Naming



All the commercially available multi-energy CTs (spectral CTs) are dual-energy CTs.

4/4/2020



The Beginning....

- "Two pictures are taken of the same slice, one at 100kV and the other at 140 kV... areas of high atomic numbers can be enhanced... Tests carried out to date have shown that iodine ($Z=53$) can be readily differentiated from calcium ($Z=20$)".
- G.N. Hounsfield, BJR 46, 1016-22, 1973.
- First widely-used commercial dual-energy CT: ~ 2005 Dual-source dual-energy CT

4/4/2020



Basic Idea

$$\begin{aligned}\mu &= f(Z, E, \rho) \\ &= \left(\frac{\mu}{\rho}\right)(Z, E) \cdot \rho\end{aligned}$$

Three variables determines linear attenuation coefficients! \implies Two measurements with known E, we can get ρ and Z. (two unknowns, two equations)

4/4/2020



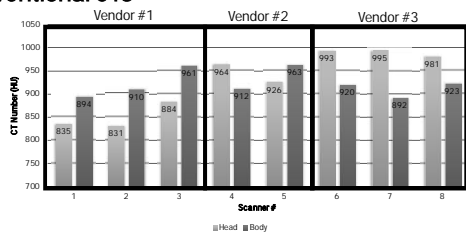
Motivations -1

- Benefits to remove E from CT images
 - Reduce artifacts: Beam hardening artifacts
 - Improve CT number consistency
 - CT numbers are affected by effective energy in CT images which depends on CT hardware, software and patient (size, location, anatomy, etc)

4/4/2020



CT Numbers of ACR Phantom Bone Insert from Conventional CTs



8 different CT Scanner models from 3 CT vendors

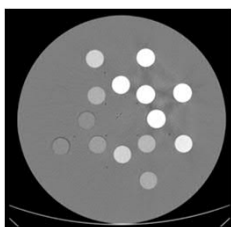
4/4/2020

Motivations - 2

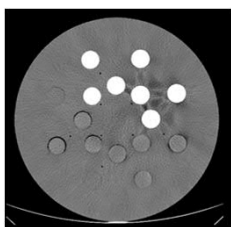
- Benefits to get ρ, Z
 - Material differentiation: materials with the same CT number may be very different, e.g., iodine and bone
 - Material qualification: ρ or ρ_e, Z ; material decomposition

4/4/2020

Calcium vs Iodine Differentiation



Conventional image (120 kV)
Iodine and calcium rods indistinguishable



Virtual non-contrast image
Only calcium rods are bright

4/4/2020

Dual-Energy CT Post-processing Models

- (ρ, Z) model – Physical effect model
 - $$\begin{cases} \mu_L = f(\rho, Z, E_L) = f_{\text{photoelectric}}(\rho, Z, E_L) + f_{\text{Compton}}(\rho, Z, E_L) \\ \mu_H = f(\rho, Z, E_H) = f_{\text{photoelectric}}(\rho, Z, E_H) + f_{\text{Compton}}(\rho, Z, E_H) \end{cases}$$
 - E_L and E_H are low and high energies determined by calibration
 - Popular in radiation therapy applications

4/4/2020

Dual-Energy CT Post-processing Models

- Basis material model – Material Decomposition
 - $$\begin{cases} \mu_L = G_L(\rho_1, \rho_2) = \rho_1 \left(\frac{\mu}{\rho}\right)_1(E_L) + \rho_2 \left(\frac{\mu}{\rho}\right)_2(E_L) \\ \mu_H = G_H(\rho_1, \rho_2) = \rho_1 \left(\frac{\mu}{\rho}\right)_1(E_H) + \rho_2 \left(\frac{\mu}{\rho}\right)_2(E_H) \end{cases}$$
 - ρ_1 and ρ_2 are density of two known (basis) materials, e.g., water and iodine, $\left(\frac{\mu}{\rho}\right)_1$ and $\left(\frac{\mu}{\rho}\right)_2$ are mass attenuation coefficients.
 - Commonly used in diagnostic imaging for material quantification

4/4/2020

Geometric Explanation of Material Decomposition

- Two material decomposition
 - $$\vec{\mu} = \rho_1 \overline{\left(\frac{\mu}{\rho}\right)_1} + \rho_2 \overline{\left(\frac{\mu}{\rho}\right)_2}$$
 - Each vector consists of low and high energy values.
 - Space (basis) change:
 - $$(\overline{\mu_L}, \overline{\mu_H}) \rightarrow \left(\overline{\left(\frac{\mu}{\rho}\right)_1}, \overline{\left(\frac{\mu}{\rho}\right)_2}\right)$$

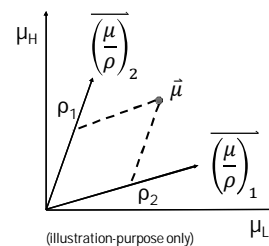


(Illustration-purpose only)

Material Quantification: Three Unknowns

- Three material decomposition
 - $\begin{cases} \mu_L = G_L(\rho_1, \rho_2, \rho_3) \\ \mu_H = G_H(\rho_1, \rho_2, \rho_3) \end{cases}$
- Underdetermined problem
 - Additional information (assumptions) required.
- Mass conservation
 - $\rho = \rho_1 + \rho_2 + \rho_3$
 - Exact, but difficult to solve the problem.
- Volume conservation
 - $1 = f_1 + f_2 + f_3$ (volume fraction)
 - Approximate, but very easy to solve.

Projection Space Decomposition

- Solving the equations using projection data
- For each projection data pair,
 - $\begin{cases} p_L = P_L(\rho_1, \rho_2) \\ p_H = P_H(\rho_1, \rho_2) \end{cases}$
 - $$P(\cdot) = \int S_L(E) \exp \left[- \int \left(\rho_1 \left(\frac{\mu}{\rho} \right)_1 + \rho_2 \left(\frac{\mu}{\rho} \right)_2 \right) ds \right] dE$$
 - Spectrum
 - Projection
- Pros
 - More accurate model than image space decomposition
 - Potentially less artifacts
- Cons
 - Computation (much) more complicated
 - No exact analytical solutions
 - Noise/error sensitive

Two Types of Dual-energy Decomposition

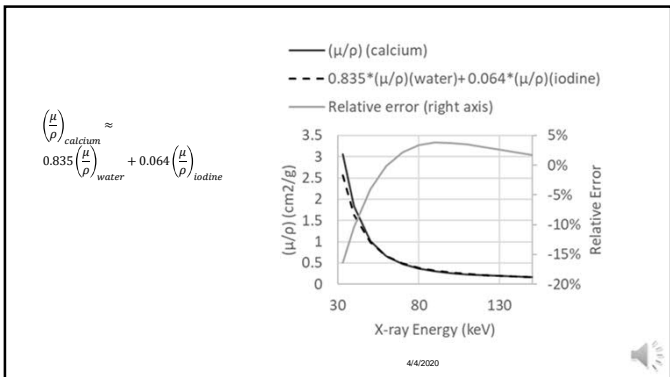
Image-space decomposition		Projection-space decomposition	
Projection data	• CT Reconstruction	Projection data	• Projection-space Decomposition
CT images	• Image-space decomposition	Basis projection data	• CT reconstruction
Spectral images	• Clinical applications	Spectral images	• Clinical applications

Interpretation of Material Decomposition Results

- $\bar{\mu} = \rho_1 \overline{\left(\frac{\mu}{\rho} \right)_1} + \rho_2 \overline{\left(\frac{\mu}{\rho} \right)_2}$
- If material $\bar{\mu}$ is made of basis materials $\overline{\mu}_1$ and $\overline{\mu}_2$, the calculated ρ_1 and ρ_2 are related to physical mass density.
- Example, do a water/iodine decomposition on a water and iodine mixture.

Interpretation of Material Decomposition Results

- $\bar{\mu} = \rho_1 \overline{\left(\frac{\mu}{\rho} \right)_1} + \rho_2 \overline{\left(\frac{\mu}{\rho} \right)_2}$
- What does it mean if material $\bar{\mu}$ is different from basis materials?
- Example:
 - $\left(\frac{\mu}{\rho} \right)_{calcium} \approx 0.835 \left(\frac{\mu}{\rho} \right)_{water} + 0.064 \left(\frac{\mu}{\rho} \right)_{iodine}$
 - The 0.835 and 0.064 can be interpreted as effective density, rather than physical density.

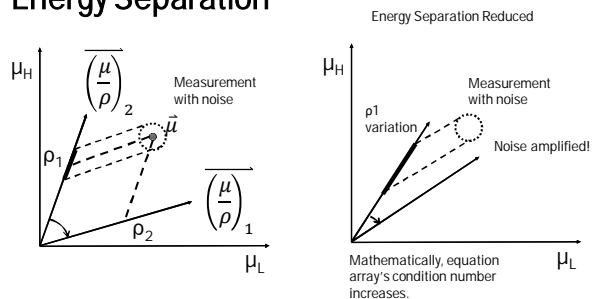


Dedicated DECT Scanners

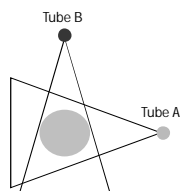
Key requirements

- Minimize the time interval between two acquisitions
 - Ideally two acquisitions simultaneously
- Maximize spectral separation – difference between two energies
 - Improve CNR

Energy Separation



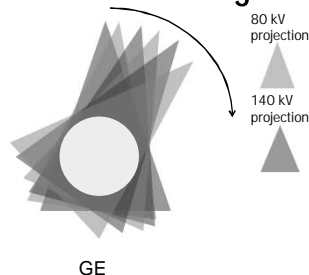
Dual-source DECT



Siemens

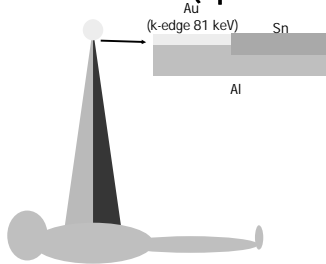
- Two tubes/detectors ~ 90° apart
- Operate independently: Two kVs/filters, tube current modulation, simultaneously low and high energy imaging
- Limitations:
 - One tube has limited field of view (up to 35.6 cm vs. 50 cm)
 - Image-space decomposition

Fast kV-switching DECT



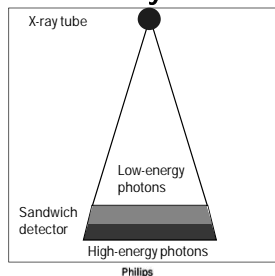
- One tube & detector system.
- Two kV fast alternating in one rotation
- Compared to dual-source CT:
 - Pros: Projection-space decomposition; full field of view for spectral imaging (50 cm)
 - Cons: No tube current modulation, same filter for low and high kVs

Twin-Beam (split filter) DECT



- Two filters on the tube: split beam into low and high energy, i.e., half detector rows acquire low/high energy images.
- Compared to other systems
 - Pros: economical
 - Cons: require powerful generator; small pitch (slow scanning)

Dual-layer Detector DECT



- Sandwich (spectral) detector: upper layer absorbs lower-energy photons and lower layer absorbs higher energy photons
- Compared to other systems:
 - Pros: conventional and spectral imaging simultaneously (work flow); projection-space decomposition; full field of view; current modulation;
 - Cons: energy separation limited by detector.

Clinical Applications

- Synthetic dual-energy CT images
 - Virtual monoenergetic images
 - Material specific / removed images for quantification and differentiation: Iodine map, Virtual noncontrast images, dual-energy ratio/slope
 - Z and ρ_e maps



Virtual Monoenergetic (monochromatic) Images

- $\mu(E_m) = \rho_1 \left(\frac{\mu}{\rho}\right)_1(E_m) + \rho_2 \left(\frac{\mu}{\rho}\right)_2(E_m)$, $E_m = 40, \dots, 190$ (200) keV, every 1 keV.
 - Note: virtual mono-E does not direct connection with acquisition spectra.
- Applications
 - Middle energy level (~ 70 keV): less beam hardening artifacts, consistent CT number; conventional image replacement.
 - Low energy level(40-60 keV): Boost contrast (iodine contrast)
 - Higher energy level (>120 keV): reduce metal artifacts



Virtual monoenergetic imaging

- Improve image quality - qualitatively

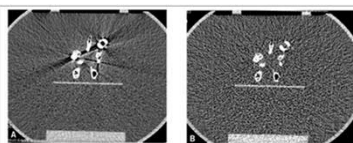


Fig. 8—Metal artifact reduction using virtual monoenergetic images synthesized from dual-source dualenergy CT data using image-space techniques. (A), Image shows pencil screw in water phantom, acquired with single-energy scan at 120 kV. (B), Monoenergetic image at 127 keV was generated from dual-energy scan with same scanner output (volume CT dose index) as used in single-energy scan. Streaking caused by metal was almost completely eliminated.

M. Bruesewitz, 2012



Large Dense Metals

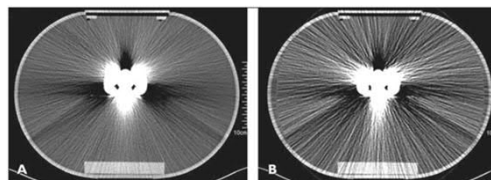


Fig. 9—Metal artifact reduction using virtual monoenergetic images synthesized from dual-source dual-energy CT is ineffective for dense metal objects.
A, Image of dense metal implant in water phantom acquired with single-energy scan at 120 kV.
B, Monoenergetic image at 127 keV generated from dual-energy scan with same scanner output (volume CT dose index) as used in single-energy scan. Streaking by metal becomes worse on virtual monoenergetic image.

Yu, 2012



Renal tumor characterization

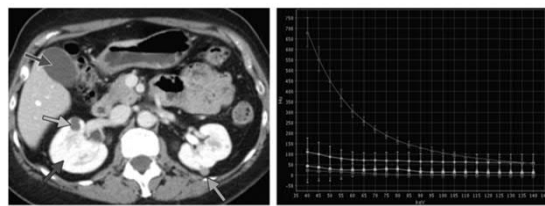


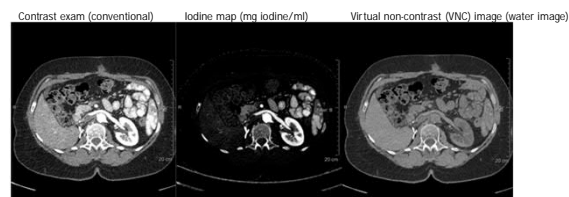
Figure 16. Simple and hemorrhagic renal cysts. (a) Monoenergetic ssDECT image shows a hyperattenuating left renal lesion (green arrow) and a hypattenuating right renal lesion (light blue arrow). The right renal lesion, with attenuation similar to that of gallbladder fluid (dark blue arrow), is likely to be a cyst.

Silva, 2011



Material specific (removed) images

- Iodine map and virtual noncontrast images



Bones in both iodine map and VNC!



DECT in Thoracic Imaging

- Pulmonary Embolism
 - Perfusion images

Figure 10. Follow-up of pulmonary embolism in a 45-year-old woman. (a) Axial weighted average image from this-section CT (3 mm section thickness) shows multilobar pulmonary embolism (arrows). (b) Axial color-coded perfusion map shows perfusion defects (arrows) in the right upper lobe and the superior segment of the left lower lobe. (c) This-section axial CT image obtained 1 month later shows marked improvement in the multilobar pulmonary embolism (arrows). (d) Axial color-coded perfusion map shows improvement in the perfusion defects in both lungs. Note the artificial perfusion defect around the superior vena cava in the anterior radio-opaque tube.

M. Kang, 2010

DECT in Abdominal Imaging

- Renal tumor/cyst
 - Patient -1
 - A: non-contrast, 120 kV
 - B: contrast, 80/140 kV
 - C: iodine map
 - Patient -2
 - D: iodine map

J. Fletcher, 2009

VNC in Abdominal Imaging

- Kidney stones
 - A: non-contrast
 - B: contrast
 - C: VNC
- Non-contrast may be unnecessary!

J. Fletcher, 2009

Material Characterization

- Kidney stone composition analysis

J. Fletcher, 2009

DECT in Abdominal Imaging

- Kidney stones

Ravi K. Kaza, 2017

DECT in MSK

- Gout imaging

K. Glazebrook, 2011

Electron Density and Effective Z

- Radiation Therapy: Proton stopping power ratio (SPR) calculation

CT number in conventional CT :

$$\mu = f(Z, E, \rho)$$

$$\text{SPR} = \text{EDR} \times \frac{\ln[2m_e c^2 \beta^2 / I_m (1 - \beta^2)] - \beta^2}{\ln[2m_e c^2 \beta^2 / I_{\text{water}} (1 - \beta^2)] - \beta^2}$$

EDR: Electron density ratio
 I_m and I_{water} are mean excitation energy,
 which is a function of effective atomic
 number.

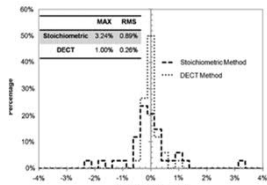


Figure 5. Histograms of relative errors in the SPRs of 34 standard human tissues (table 1) estimated using the stochastic calibration method and the DECT method.

M. Yang, et al. 2010

Electron Density and Effective Z

- Tissue segmentation for MC dose calculation

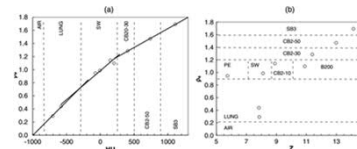


Figure 4. Tissue segmentation for MC dose calculations in phantoms B and C using single-energy CT images (a) and dual-energy CT images (b).

M Bazalova, et al. PBM 2008

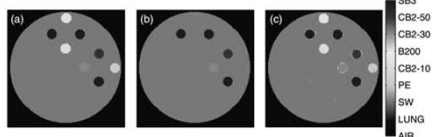


Figure 8. Material segmentation for electron and orthovoltage photon beam dose calculations: the exact geometry (a), the single-energy CT material segmentation (b) and the dual-energy CT material segmentation (c).

M Bazalova, et al. PBM 2008

DECT Exam Considerations

- Dual-source DECT (Siemens)
 - Small FOV
 - Large patients (Low kV beam: 80/100 kV)
- Fast kV switching DECT (GE)
 - Large patients (80 kV)
 - Tube current modulation (GSI assist)
- Dual-layer detector DECT
 - Less restriction – Same protocol as conventional CT

Learning Objective

- Understand the basic physics of dual-energy CT imaging.
- Learn about the common dual-energy CT platforms and their pros and cons.
- Learn about the common dual-energy CT clinical applications.

4/4/2020

Take-home Messages

- Synthetic dual-energy CT images provide improved quality and new information.
 - We need to correctly understand the new image types, e.g., why bones show in iodine map and water (VNC) images.
- Each types of dual-energy CT scanners have its pros and cons.
- Many clinical applications have been used in clinical practice and more are coming!

UT Southwestern
Medical Center
Radiology

Xinhui Duan, PhD, DABR
Email: Xinhui.duan@utsouthwestern.edu

